Journal of Experimental Botany, Vol. 58, No. 15/16, pp. 4131–4146, 2007
doi:10.1093/jxb/erm271 Advance Access publication 7 December, 2007
This paper is available online free of all access charges (see http://jxb.oxfordjournals.org/open_access.html for further details)

Journal of Experimental Botany
www.jxb.oxfordjournals.org

RESEARCH PAPER

Tissue specialization at the metabolite level is perceived during the development of tomato fruit

Sofia Moco[1,2,3,*,†], Esra Capanoglu[2,4,*], Yury Tikunov[2,3], Raoul J. Bino[2,3,5], Dilek Boyacioglu[4], Robert D. Hall[2,3], Jacques Vervoort[1,3] and Ric C. H. De Vos[2,3]

[1] *Laboratory of Biochemistry, Wageningen University, Dreijenlaan 3, 6703 HA, Wageningen, The Netherlands*

[2] *Plant Research International, PO Box 16, 6700 AA, Wageningen, The Netherlands*

[3] *Centre for BioSystems Genomics, PO Box 98, 6700 AB Wageningen, The Netherlands*

[4] *Food Engineering Department, Faculty of Chemical and Metallurgical Engineering, Istanbul Technical University, Maslak, TR-34469 Istanbul, Turkey*

[5] *Laboratory of Plant Physiology, Wageningen University, Arboretumlaan 4, 6703 BD Wageningen, The Netherlands*

Received 30 August 2007; Revised 4 October 2007; Accepted 8 October 2007

Abstract

Fruit maturation and tissue differentiation are important topics in plant physiology. These biological phenomena are accompanied by specific alterations in the biological system, such as differences in the type and concentration of metabolites. The secondary metabolism of tomato (*Solanum lycopersicum*) fruit was monitored by using liquid chromatography (LC) coupled to photo-diode array (PDA) detection, fluorescence detection (FD), and mass spectrometry (MS). Through this integrated approach different classes of compounds were analysed: carotenoids, xanthophylls, chlorophylls, tocopherols, ascorbic acid, flavonoids, phenolic acids, glycoalkaloids, saponins, and other glycosylated derivatives. Related metabolite profiles of peel and flesh were found between several commercial tomato cultivars indicating similar metabolite trends despite the genetic background. For a single tomato cultivar, metabolite profiles of different fruit tissues (vascular attachment region, columella and placenta, epidermis, pericarp, and jelly parenchyma) were examined at the green, breaker, turning, pink, and red stages of fruit development. Unrelated to the chemical nature of the metabolites, behavioural patterns could be assigned to specific ripening stages or tissues. These findings suggest spatio-temporal specificity in the accumulation of endogenous metabolites from tomato fruit.

Key words: Fluorescence detection, fruit tissues, liquid chromatography, mass spectrometry, metabolomics, photo-diode array, ripening, tomato fruit.

Introduction

Tomato or *Solanum lycopersicum* (formerly *Lycopersicum esculentum*) is part of the *Solanum* family which contains many other plant species of commercial and/or nutritional interest (e.g. potato, pepper, eggplant, tobacco, and petunia). The tomato fruit is one of the most widely grown fruits for consumption, with more than 122 million tons being produced worldwide in 2005 (FAOSTAT, 2005). There are several quality aspects associated with the nutritional value of the tomato fruit, as well as with the profile of flavour volatiles, flavonoids, vitamins, and carotenoids, all of which are of relevance for market consumption. The tomato fruit is an important natural source of lycopene, a carotenoid, which has been the subject of recent controversy due to alleged beneficial effects on, for example, prostate cancer prevention (Basu and Imrhan, 2007; Jatoi *et al*., 2007).

Besides the nutritional value inherent in the tomato and the proposed health benefits, the tomato fruit is the most well studied of all fleshy fruits and represents a model of choice for developmental studies. During fruit ripening, a series of physiological phenomena occur such as alterations in pigment biosynthesis, decrease in resistance

* These authors contributed equally to this work.
† To whom correspondence should be adrressed. E-mail: sofia.moco@wur.nl

© 2007 The Author(s).
This is an Open Access article distributed under the terms of the Creative Commons Attribution Non-Commercial License (http://creativecommons.org/licenses/by-nc/2.0/uk/) which permits unrestricted non-commercial use, distribution, and reproduction in any medium, provided the original work is properly cited.

Downloaded from https://academic.oup.com/jxb/article/58/15-16/4131/449422 by U.S. Department of Justice user on 17 August 2022

to pathogen infection, modification of cell wall structure, conversion of starch to sugars, and increase of the levels of flavour and aromatic volatiles (Fraser *et al*., 1994; Giovannoni, 2001; Carrari *et al*., 2006). In climacteric fruits, such as the tomato fruit, ethylene plays a major role in fruit development and ripening, in addition to other plant hormones such as auxin and abscisic acid, as well as gibberellins and cytokinins (Srivastava and Handa, 2005). However, the dynamics and interactions within fruit metabolic pathways, as well as the identity and concentrations of the interacting metabolites during fruit development, are mostly unknown.

Metabolomics facilitates the diagnosis of plant status by having a direct relationship to the exhibited visual characteristics (phenotype). Using metabolomics technologies, a comprehensive description of naturally-occurring metabolites (primary and secondary metabolites) in a biological system, such as tomato fruit, is now feasible. The recent expansion of metabolomic technologies has resulted in the broader use of a diverse range and configuration of instruments and analytical methods. Mostly MS (Schauer *et al*., 2005; Tikunov *et al*., 2005; van der Werf *et al*., 2005; Moco *et al*., 2006; Fraser *et al*., 2007) and NMR (Keun *et al*., 2002; Le Gall *et al*., 2003; Ward *et al*., 2003; Kochhar *et al*., 2006; Griffin and Kauppinen, 2007) technologies are used, but also other techniques such as LC-photo-diode array (PDA) (Porter *et al*., 2006), infrared and Raman spectroscopy (Ellis and Goodacre, 2006) have been used for plant metabolomics. Among a wide variety of applications (Hall, 2006; Schauer and Fernie, 2006), plant metabolomics approaches are providing insight into the biochemical composition of the plant system, allowing the establishment of links to possible metabolite functions.

The description of metabolites in biological systems depends not only on technological developments in analytical methods, but also on the capacity to sort and store relevant information for re-use in related research. The integration of experimental data (e.g. mass spectrum, fragmentation pattern, NMR spectrum, retention time in a described separation system, UV/Vis spectrum) with both biological (e.g. species name, organ, tissue) and chemical (e.g. name, chemical descriptors, molecular formula, structure) information can greatly improve and optimize the ability to describe metabolites in their biochemical context. Therefore, major efforts are being made towards the management of metabolite information by means of databases (Ogata *et al*., 1999; Kopka *et al*., 2005; Moco *et al*., 2006; Oikawa *et al*., 2006; Choi *et al*., 2007; Wishart *et al*., 2007). The development of such databases can lead to a better understanding of biochemical composition and contributes to a greater overall insight into the functioning of the biological system. Consequently, interpretation of complex metabolic transformation processes, as occurs during fruit development, can benefit from (already available) database information, avoiding the need of intense identification efforts.

Within the multiplicity of metabolites that constitutes the tomato fruit metabolome, carotenoids, flavonoids, phenolic acids, and alkaloids can be analysed using LC-PDA/MS techniques. A variety of biological functions have been assigned to these classes of secondary metabolite, for example, as components involved in pollination, photoprotection, seed dispersal, adaptation to abiotic conditions, and defence, as well as being involved in other non-ecological phenomena such as auxin transport (Tracewell *et al*., 2001; Friedman, 2002; Taylor and Grotewold, 2005; Kunz *et al*., 2006; Simons *et al*., 2006). Furthermore, biochemical studies on crops, including tomato fruit, may generate knowledge that potentially can have a direct consumer impact as it provides insight into nutritional and quality aspects.

Using metabolomics analyses based on LC-QTOF (quadrupole time-of-flight)-MS, peel and flesh tissues of the tomato cultivar *Moneymaker* have recently been compared and it was shown that specific metabolites could be attributed to both these tissues (Moco *et al*., 2006). For instance, all flavonoids and α-tomatine were mainly found in the peel, while tomatoside A, a hydroxyfurostanol-tetrahexose, was uniquely present in the flesh (including seeds). In the present study, fruit tissues from a range of tomato cultivars and at different ripening stages have been compared in terms of their metabolite profiles using both LC-QTOF MS and LC-PDA-FD. The combination of different analytical methods resulted in the detection of a large variety of metabolites (including isoprenoids, ascorbic acid, phenolic acids, flavonoids, saponins, and glycoalkaloids) and provided novel insight into tissue-specificity within ripening tomato fruit.

Materials and methods

Plant materials

Fruits from seven cultivars of tomato (*Solanum lycopersicum*, cultivars *Conchita*, *Campari*, *Favorita*, *Macarena*, *Cedrico*, *Aromata*, and *Celine*), at the red stage of development were acquired from local supermarkets, while fruits of the cultivar *Moneymaker* were harvested from plants grown in the greenhouse at Wageningen University. From these fruits, the peel was separated from the rest of the fruit (flesh) and both fruit tissues were immediately frozen in liquid nitrogen. The frozen material was ground to a fine powder and stored at –80 °C before analysis. Both the peel and flesh tissues of these cultivars were used for metabolite profiling using LC-MS (Moco *et al*., 2006).

For the single tomato cultivar, *Ever*, fruits were also harvested at different stages of development, i.e. green, breaker, turning, pink, and red, from plants grown in an environmentally controlled greenhouse located at Wageningen University. Tissues were collected from: the vascular attachment region (VAR), epidermis (EP), pericarp (PR), columella and placenta (CP), and jelly parenchyma (JE) (including the seeds), using 10 fruits for each developmental stage. After collection, all tissue samples were immediately frozen in liquid nitrogen. After grinding the frozen

Downloaded from https://academic.oup.com/jxb/article/58/15-16/4131/449422 by U.S. Department of Justice user on 17 August 2022

tomato material in liquid N_2, these different tissue samples were freeze-dried and the final water content was determined (Horwitz, 2000). These samples were analysed and quantified firstly for the occurrence of specific metabolites (isoprenoid derivatives and ascorbic acid) using LC-PDA-FD and were then also profiled for semi-polar metabolites using LC-MS. Seeds of variety *Moneymaker* were harvested from red fruits and treated using 0.1 M hydrochloric acid followed by extensive washing with water and air-drying. Seeds from variety *Ever* were kindly provided by Seminis (Wageningen, The Netherlands).

Chemicals

The standard compounds: chlorogenic acid, β-carotene, lutein, all *trans*-lycopene (from tomato, 90–95%), chlorophyll *a* and *b* from spinach, α-, δ-, and γ-tocopherol were purchased from Sigma (St Louis, USA), naringenin from ICN (Ohio, USA), rutin from Acros (New Jersey, USA), naringenin chalcone from Apin Chemicals (Abingdon, UK), ascorbic acid from Merck (Darmstadt, Germany), neoxanthin and violaxanthin from CaroteNature (Lupsingen, Switzerland), and lutein from Extrasynthese (Genay, France). The solvents acetonitrile, methanol, and chloroform were of HPLC supra gradient quality and obtained from Biosolve (Valkenswaard, The Netherlands) and ethyl acetate (for HPLC) from Acros (New Jersey, USA). *Tris*(hydroxymethyl)methylamine (TRIS) was obtained from Invitrogen (Carlsbad, USA). Metaphosphoric acid ($(HPO_3)n$), sodium chloride (NaCl), diethylene triamine pentaacetic acid (DTPA), butylated hydroxytoluene (BHT), and leucine enkaphaline were obtained from Sigma (St Louis, USA). Formic acid (FA) for synthesis, 98–100%, was purchased from Merck-Schuchardt (Hohenbrunn, Germany), monopotassium phosphate (KH_2PO_4) pro analysis and hydrochloric acid were obtained from Merck (Darmstadt, Germany), and dipotassium phosphate (K_2HPO4) 98% from Sigma (St Louis, USA). Ultra pure water was obtained from an Elga Maxima purification unit (Bucks, UK).

Extraction, separation, and detection of isoprenoid derivatives

The extraction of lipid-soluble isoprenoids was performed according to Bino *et al.* (2005) using 25±0.05 mg of freeze-dried tomato material. Three extractions of the same material were made for each analysis. For chromatographic separation the extracts (10 µl) were injected into a LC-PDA-FD system composed of a W600 pump system (Waters Chromatography, Milford, MA, USA) equipped with a YMC-Pack reverse-phase C30 column (250×4.6 mm, particle size 5 µm), maintained at 40 °C. Eluting compounds were detected using a Waters 996 PDA detector over the UV/Vis range of 240 to 750 nm coupled online to a Waters 2475 fluorescence detector. Data were analysed using Empower Pro software (2002; Waters). Measurements for neoxanthin and violaxanthin were made at 440 nm, chlorophyll *b* at 470 nm, β-carotene, lutein, and lycopene at 478 nm, and chlorophyll *a* at 665 nm. α-, δ-, and γ-tocopherols were analysed using fluorescence detection with excitation at 296 and emission at 340 nm. The quantification of isoprenoids was based on calibration curves constructed from injecting known amounts of the respective standard compounds.

Extraction, separation, and detection of ascorbic acid

For the analysis of ascorbic acid, a 5% (m/v) $(HPO_3)n$ with 1 mM aqueous DTPA was prepared as extraction solution (continuous stirring and sonication was needed to obtain a homogeneous solution). This solution was stored at 4 °C before analysis. To 25±0.05 mg freeze-dried tomato tissue, 0.475 ml water was added, immediately followed by 2 ml ice-cold extraction solution. The extracts were stirred and left on ice before 15 min sonication. After centrifugation at 2500 rpm for 10 min, the supernatants were filtered through 0.2 µm polytetrafluoroethylene filters and taken for LC-PDA analysis. The same LC-PDA system was used as for the analysis of isoprenoids. Separation was performed at 30 °C on a YMC-Pack Pro C18 (150×4.6 mm, 5 µm particle size) column using 50 mM phosphate buffer (pH 4.4) as mobile phase. After 15 min separation, the column was washed with acetonitrile and reconditioned for the injection of the next sample. The detection and quantification of ascorbic acid was made at 262 nm by means of a calibration curve.

Extraction, separation, and detection of semi-polar metabolites

For the analysis of the cultivars *Conchita*, *Campari*, *Favorita*, *Macarena*, *Cedrico*, *Aromata*, *Celine*, and *Moneymaker*, 0.5 g fresh weight tomato powder was extracted with 1.5 ml methanol, following the protocol described by Moco *et al.* (2006). For the analysis of the fruit tissues from the cultivar *Ever*, the same procedure was applied using 25±0.05 mg freeze-dried material and 2 ml of 75% methanol (in three replicates). The seeds of *Ever* and *Moneymaker* were also extracted using this procedure using 50±0.05 mg in 2 ml. The extracts obtained were taken for LC-PDA-QTOF MS analysis in electrospray negative mode (ESI^-), as previously described by Moco *et al.* (2006). In brief, a Waters Alliance 2795 HT system equipped with a Luna C18(2) pre-column (2.0×4 mm) and analytical column (2.0×150 mm, 100 Å, particle size 3 µm) from Phenomenex (Torrance, CA, USA) were used for chromatographic separation. Degassed solutions of formic acid:ultra pure water (1:1000, v/v) (eluent A) and formic acid:acetonitrile (1:1000, v/v) (eluent B) were pumped at 0.19 ml min^{-1} into the HPLC system. The gradient used started at 5% B and increased linearly to 35% B in 45 min. The next injection started after 15 min of washing and equilibration of the column. The column temperature was kept at 40 °C and the samples at 20 °C. The room temperature was maintained at 20 °C. The HPLC system was connected online to a Waters 2996 PDA detector and subsequently to a QTOF Ultima V4.00.00 mass spectrometer (Waters-Corporation, MS technologies, Manchester, UK). For LC-MS measurements 5 µl of sample (methanolic extract) was injected into the system and for LC-MS/MS 10 µl. The MS/MS measurements were made with increasing collision energies according to the following program: 10, 15, 25, 35, and 50 eV. Leucine enkaphalin ($[M-H]^-$ =554.2620) was injected through a separate inlet and used as 'lock mass'.

Data analysis and alignment

Acquisition, visualization, and manual processing of LC-PDA-MS/MS data were performed under MassLynx™ 4.0 (Waters). Mass data were automatically processed by metAlign version 1.0 (www.metAlign.nl). Baseline and noise calculations were performed from scan number 70 to 2400, corresponding to retention times 1.4 min to 48.6 min. The maximum amplitude was set to 35 000 and peaks below twice the local noise were discarded. More details about the settings of metAlign can be found elsewhere (De Vos *et al.*, 2007).

Annotation of metabolites

The obtained datasets were analysed as [retention time×accurate mass×peak intensity] matrixes for metabolite identification. The matrix was reduced by discarding all signals below a signal intensity of 100 (ion counts per scan at the centre of the peak) and those eluting within the first 4 min of chromatography. This dataset was then checked for the presence of known tomato fruit metabolites using the MoTo DB (http://appliedbioinformatics.wur.nl/moto), after manually calculating the accurate masses by taking into account a mass signal intensity ratio of analyte versus

Downloaded from https://academic.oup.com/jxb/article/58/15-16/4131/449422 by U.S. Department of Justice user on 17 August 2022

lock mass of 0.25–2.0 (Moco *et al*., 2006). For mass signals lower than 0.25×lock mass intensity it was impossible to calculate a correct and accurate mass. To annotate compounds, the tolerance for mass deviation was set at 5 ppm, taking into account the correct analyte/lock mass ratio. For an observed accurate mass, a list of possible molecular formulae was obtained, selected for the presence of C, H, O, and N, S or P. In addition, raw datasets were checked manually in MassLynx software for retention time, UV/Vis spectra and QTOF-MS/MS-fragmentation patterns for chromatographically separated peaks not present in the MoTo DB, to complement the accurate mass-based elemental formulas.

Multivariate analyses of LC-MS and LC-PDA-FD data

For the comparison and visualization of the main tendencies of the LC-MS data acquired for the peel and flesh tissues of the eight cultivars, the data matrix obtained from metAlign was loaded into GeneMaths software (Applied Maths, Belgium). Principal components analysis was performed after logarithmic (of base 2) transformation and standardization across the samples using range scaling (Smilde *et al*., 2005).

The LC-MS derived dataset from the tissues of *Ever* at different ripening stages after processing by metAlign initially consisted of about 20 000 mass signals aligned across all samples analysed. The means of replicate samples were calculated and used in the further data analysis. Low intensity mass signal patterns were discarded (as described above), thereby reducing the data set to 10 388 mass peaks. Most compounds are usually represented by a number of ions (isotopes and unintended fragments and adducts) that makes the entire LC-MS data highly redundant. This redundancy was removed by clustering of mass peak patterns using an approach called Multivariate Mass Spectra Reconstruction (Tikunov *et al*., 2005). This resulted in 504 mass peak clusters, each of which was represented by a single mass signal in further analyses. A small dataset containing the quantified levels of carotenoids, tocopherols, chlorophylls, and ascorbic acid, analysed by LC-PDA-FD, was appended to the LC-MS data resulting in a final data set comprising 528 components (variables). Each variable was normalized across the samples using range scaling (Smilde *et al*., 2005). The normalized data were subjected to an unsupervised clustering using Self Organizing Tree Algorithm (SOTA) (Herrero *et al*., 2001). Fourteen clusters with significant internal variability (P <0.001) were derived using this procedure.

Results

The metabolites in tomato fruit extracts have been analysed by different LC-hyphenated methods in order to profile a wide variety of compounds naturally occurring in tomato fruit and to establish differences between different fruit tissues and ripening stages. To assess the tissue specificity of metabolites, fruits from a series of tomato cultivars were separated into peel and flesh, followed by a more detailed study on a single cultivar using a finer separation of the fruit tissues at different stages of development.

LC-MS analyses of peel and flesh from different tomato cultivars

The specificity of metabolite accumulation in two fruit tissues (peel and flesh) has been tested previously for one tomato cultivar, *Moneymaker*, at the red stage of fruit development. The peeled EP was classified as 'peel' and the rest of the fruit (including the seeds) was classified as 'flesh' (Moco *et al*., 2006). In the present study these two tissues were also analysed for other tomato cultivars, taken also at the red stage of development. The cultivars chosen (*Conchita*, *Campari*, *Favorita*, *Macarena*, *Cedrico*, *Aromata*, and *Celine*) are all commercial cultivars widely available for consumption. Three replicates of 75% methanolic extracts of the same biological material per cultivar and per tissue were analysed using LC-PDA-QTOF-MS.

Firstly, the extraction procedure and the LC-MS measurements were tested for reproducibility. The standard error of the means of three replicate measurements of the same extract was 5.2%, which indicates a high technical reproducibility of the LC-MS analyses. The overall standard error of the replicate (n=3) mass signal intensity means of extracts prepared from the same biological material was 6.8%, indicating that the extraction procedure was also highly reproducible.

Secondly, in order to compare the LC-MS profiles of the different tomato cultivars, including *Moneymaker*, a principal components analysis (PCA) was performed (Fig. 1). The x-axis of the PCA plot (first component) coincided with the separation of peel and flesh, while the y-axis (second component) corresponded to the different cultivars. This result supports a stronger tissue-driven variation than a cultivar-driven variation. This means that the metabolite profiles of the same fruit tissue in different

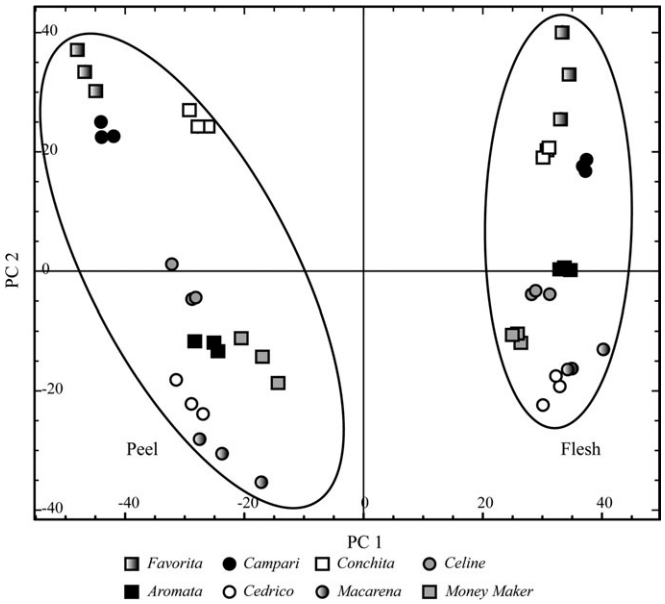

Fig. 1. Principal component analysis (1st principal component, PC1, versus 2nd principal component, PC2) of the tomato fruit tissues peel and flesh of different cultivars: *Favorita*, *Campari*, *Conchita*, *Cedrico*, *Aromata*, *Celine*, *Macarena*, and *Moneymaker* for three replicate extractions (explained variance in the x-axis, PC1, 22.2% and in the y-axis, PC2, 9.6%).

Downloaded from https://academic.oup.com/jxb/article/58/15-16/4131/449422 by U.S. Department of Justice user on 17 August 2022

cultivars are more similar than the profiles of the two different tissues within each cultivar. The metabolite putatively annotated as tomatoside A (Moco *et al.*, 2006) was one of the main signals responsible for the separation of the flesh from the peel tissues for all the analysed tomato cultivars, while flavonoids appeared as metabolites specific for peel tissue.

Tissue specificity of metabolites during fruit ripening

In order to evaluate the tissue distribution of metabolites upon ripening, fruits from a single tomato cultivar, *Ever*, were chosen for more extensive analysis. For this purpose, fruits at five ripening stages were divided into five different tissues. From the outside to the centre of the fruit, the following fruit parts were separated and analysed individually: the area of the fruit below the abscission zone connecting the fruit and the pedicel (VAR), the external (epidermal) tissue layer (exocarp or EP), the fleshy tissue layer below the EP (PR), the gelatinous locular tissue of the fruit including the seeds (JE), and the central inner fleshy tissue of fruit (CP) (Fig. 2F). All these tissues were analysed for their metabolite profiles using both LC-PDA-FD and LC-PDA-QTOF-MS.

During ripening of the tomato fruit, changes in pigmentation are evident through the different developmental stages chosen for the analyses, from the stage green, passing through breaker, turning, pink, and finally reaching red (ripe) fruit stage (Fig. 2A–E). However, throughout the period chosen, no obvious changes in fruit size were observed between the developmental stages analysed.

Fig. 2. Fruit ripening stages of the tomato cultivar *Ever*: green (A), breaker (B), turning (C), pink (D), and red (E) and different tissues within the fruit: vascular attachment region (VAR; 1), epidermis (EP; 2), jelly parenchyma (including the seeds) (JE; 3), columella and placenta (CP; 4), and pericarp (PR; 5).

Isoprenoids and ascorbic acid in fruit tissues during ripening

The amounts of specific isoprenoids were determined in the different fruit tissues and in the diffierent ripening stages of tomato, using LC-PDA-FD (Table 1). The tendencies observed during development were similar for all tissues: there was an increase in lycopene during fruit development and a decrease in chlorophylls (*a* and *b*). This was also obvious from the changes in fruit colour (from a green to a red coloured-fruit). β-Carotene increased, neoxanthin slightly decreased, while lutein was virtually constant during development. Violaxanthin showed a profile that was slightly different from the other xanthophylls. This compound first increased up to breaker/pink stage and then decreased to the red stage. In general, the α-, γ-, and δ-tocopherols increased during ripening in all tissues except the JE, in which all tocopherols decreased.

Clear differences were observed in the levels of isoprenoids between the different tissues, as well as in the increase or decrease in the rate of change during development. Lycopene increased mostly in the EP: more than 20 000-fold from the green to the red stage (up to about 2.5 mg g^{-1} dry weight). Chlorophyll *a* was higher than chlorophyll *b*, with a ratio of *c*. 3 in all tissues. Both chlorophyll forms were most abundant in the VAR and the JE, while lowest levels were detected in the CP and EP. The amount of β-carotene ranged from 4 (green CP) to 85 (red EP) μg g^{-1} dry weight. In green fruits, the xanthophylls were highest in the JE, while in red fruits they were highest in the VAR. Low amounts of neoxanthin occurred in all tissues of tomato remaining <15 μg g^{-1} dry weight. The levels of violaxanthin were relatively stable during development of all tissues. Lutein was least abundant in the EP and reached the highest levels in the VAR at all developmental stages.

The tocopherols were present at different concentrations in diverse parts of the tomato fruit. Vitamin E (α-tocopherol) was the most abundant tocopherol in all tissues and at all developmental stages, being highest in the VAR and lowest in the PR. γ-Tocopherol, which is the biosynthetic precursor of α-tocopherol, was highest in the JE of the tomato fruit. The ratio α- versus γ-tocopherol clearly differed between tissues, suggesting tissue-dependent differences in the activity of the corresponding γ-tocopherol methyltransferase. The levels of δ-tocopherol were relatively low in all tissues (but highest in the red

Downloaded from https://academic.oup.com/jxb/article/58/15-16/4131/449422 by U.S. Department of Justice user on 17 August 2022

Table 1. *Water content (W), in %, and levels, in μg g^{-1} dry weight, of isoprenoid derivatives (neoxanthin, violaxanthin, β-carotene, all trans-lycopene, lutein, chlorophyll a, chlorophyll b, α-tocopherol, δ-tocopherol, γ-tocopherol) and ascorbic acid in the tissues of tomato fruit (VAR, CP, EP, PR, and JE), at different ripening stages (green, breaker, turning, pink, and red), represented as means ±standard error of the means (n=3)*

Ripening stages[a]	W (%)	Neoxanthin	Violaxanthin	β-Carotene	All *trans*-lycopene	Lutein	Chlorophyll *a*	Chlorophyll *b*	δ-Tocopherol	γ-Tocopherol	α-Tocopherol	Ascorbic acid
						VAR						
G	94	11.81±1.31	20.93±0.47	10.32±1.70	1.91±0.48	34.12±4.27	254.56±23.51	96.32±10.70	0.22±0.02	10.19±0.16	406.29±9.39	274.09±2.83
B	93	10.68±0.81	27.01±0.35	20.07±3.70	4.96±0.80	34.02±0.89	214.12±19.65	69.37±6.63	1.08±0.00	15.42±0.20	483.93±15.60	796.03±2.31
T	94	10.97±0.69	36.44±0.10	38.12±5.39	48.86±8.25	36.63±1.18	166.13±11.84	53.40±3.59	2.60±0.07	32.09±0.47	554.89±7.49	412.44±6.73
P	94	8.46±0.42	32.68±0.19	52.25±5.48	110.15±18.02	30.06±0.44	108.02±5.01	30.60±2.38	2.84±0.04	37.91±0.81	631.76±9.76	415.60±3.47
R	94	5.51±0.27	22.87±0.67	74.03±3.89	400.83±35.19	30.77±0.67	49.13±2.02	14.29±1.29	3.23±0.09	62.73±1.13	537.59±3.40	1286.85±5.84
						CP						
G	94	6.25±0.40	12.19±0.24	4.17±0.56	nd[b]	16.28±0.99	98.06±6.85	37.47±2.09	0.03±0.02	3.11±0.11	209.03±1.36	146.56±2.51
B	94	4.91±0.19	20.29±0.42	21.81±1.77	20.22±1.09	18.24±1.28	51.40±3.37	18.32±1.59	0.44±0.01	7.34±0.06	210.75±2.79	549.76±3.20
T	95	5.73±0.56	22.8±0.40	28.15±3.82	35.68±4.51	15.85±0.60	45.95±7.42	15.99±1.24	0.82±0.01	10.05±0.14	278.47±2.66	701.97±3.37
P	94	4.04±0.45	21.43±0.35	43.84±2.47	110.26±7.53	11.42±0.24	15.73±1.46	7.52±0.92	0.83±0.01	9.99±0.12	279.53±2.47	869.48±6.38
R	95	3.62±0.44	23.95±0.33	60.98±3.10	253.98±16.29	12.24±0.61	nd	2.23±0.50	1.06±0.00	15.34±0.34	316.95±1.13	1302.36±5.08
						EP						
G	94	2.01±0.46	8.55±0.45	7.64±0.12	nd	9.15±1.27	102.56±7.22	26.07±0.67	1.76±0.03	33.67±0.31	181.19±5.54	1176.59±7.24
B	94	3.13±0.56	15.71±0.87	23.61±1.53	40.18±3.24	11.35±1.20	81.02±5.15	20.56±1.74	3.27±0.06	41.55±1.54	193.69±7.94	1609.36±10.28
T	94	1.7±0.16	13.23±0.94	39.54±0.46	214.69±2.32	8.95±0.56	24.4±1.49	3.75±0.45	5.86±0.04	62.11±0.34	208.25±5.31	1553.45±5.96
P	94	1.8±0.21	6.47±0.49	64.89±1.78	874.25±23.38	8.58±0.13	5.03±0.51	1.28±0.08	7.38±0.05	77.38±0.73	214.31±1.89	1616.4±3.27
R	93	nd	9.92±0.14	84.64±4.54	2786.53±86.83	9.04±0.38	nd	nd	7.57±0.11	69.11±1.21	193.69±3.26	1670.74±7.61
						PR						
G	95	6.34±0.56	11.39±0.08	8.29±0.23	0.48±0.04	18.08±0.54	121.83±13.37	43.41±4.03	2.72±0.57	77.32±25.33	155.40±11.52	703.75±2.48
B	95	6.73±0.62	16.84±0.31	29.15±0.33	41.58±1.22	25.36±0.50	73.10±6.25	23.54±3.33	6.16±0.22	151.07±5.64	157.54±5.72	1174.49±8.25
T	95	2.91±0.61	11.96±1.18	44.66±6.89	78.44±33.75	21.37±0.60	27.57±2.74	8.49±0.70	5.19±0.16	128.69±4.63	165.18±1.71	1404.24±10.97
P	96	3.09±0.20	11.00±1.32	50.03±5.68	301.50±9.98	20.90±0.78	6.65±0.26	3.34±0.05	4.66±0.16	85.58±2.81	195.60±3.80	1141.82±7.67
R	95	nd	5.48±0.09	49.9±1.83	845.68±17.21	14.16±0.45	nd	nd	4.33±0.13	129.74±6.14	216.62±7.06	1517.8±6.08
						JE						
G	94	13.57±1.57	25.09±0.77	15.21±0.59	nd	39.73±1.44	281.95±8.1	119.37±9.09	3.07±0.51	102.11±22.16	133.02±8.58	830.34±12.8
B	93	4.62±0.12	17.83±1.61	64.90±4.35	115.02±7.44	25.75±1.01	21.78±3.34	5.48±0.82	1.02±0.00	13.37±0.21	121.36±1.60	1040.81±11.57
T	94	2.90±0.38	13.29±0.59	73.99±1.59	213.18±5.47	20.23±0.21	2.39±1.43	0.86±0.43	1.37±0.00	21.61±1.19	132.45±2.41	1108.41±8.82
P	93	2.63±0.20	12.88±0.77	73.74±4.11	366.83±16.84	21.16±0.96	0.96±0.96	nd	1.42±0.00	25.28±0.96	136.40±1.80	1039±7.24
R	94	1.93±0.32	8.34±0.40	69.27±2.41	542.63±21.10	21.46±1.09	0.32±0.32	nd	1.52±0.01	22.22±0.31	114.29±0.54	1141.90±8.36

[a] Ripening stages: G, green; B, breaker; T, turning; P, pink; R, red.
[b] nd, Not detectable (<1 μg g^{-1} dry weight).

Downloaded from https://academic.oup.com/jxb/article/58/15-16/4131/449422 by U.S. Department of Justice user on 17 August 2022

EP), while β-tocopherol was not detectable at all (less than 0.1 μg g^{-1} dry weight).

The level of ascorbic acid (vitamin C) increased during ripening in all tissues, though its increase was generally largest between green/breaker or breaker/turning (Table 1). In the VAR, vitamin C displayed a rather specific pattern upon fruit ripening: a nearly 3-fold increase from green to breaker, followed by a 2-fold decrease from breaker to turning and again a 3-fold increase from pink to red stage. When red fruit are compared to green fruit, ascorbic acid increased nearly 10-fold in the CP and <2-fold in the EP. However, at all ripening stages, the highest levels of this antioxidant were detected in the EP fraction of the fruits.

Semi-polar metabolites in the fruit tissues during ripening

The LC-PDA-QTOF-MS analysis of metabolites present in the semi-polar extracts, over a definite range of polarity as imposed by the reversed-phase column used for the analytical separation, allowed the detection of mostly glycosylated derivatives of phenolic acids, flavonoids, alkaloids, and other small molecules. The different fruit tissue profiles were quite diverse, as shown by the mass chromatograms obtained (Fig. 3). It was also evident that, in all tissues, marked changes in metabolites occurred during ripening of the fruit. This involved both the complete disappearance as well as the appearance of mass signals.

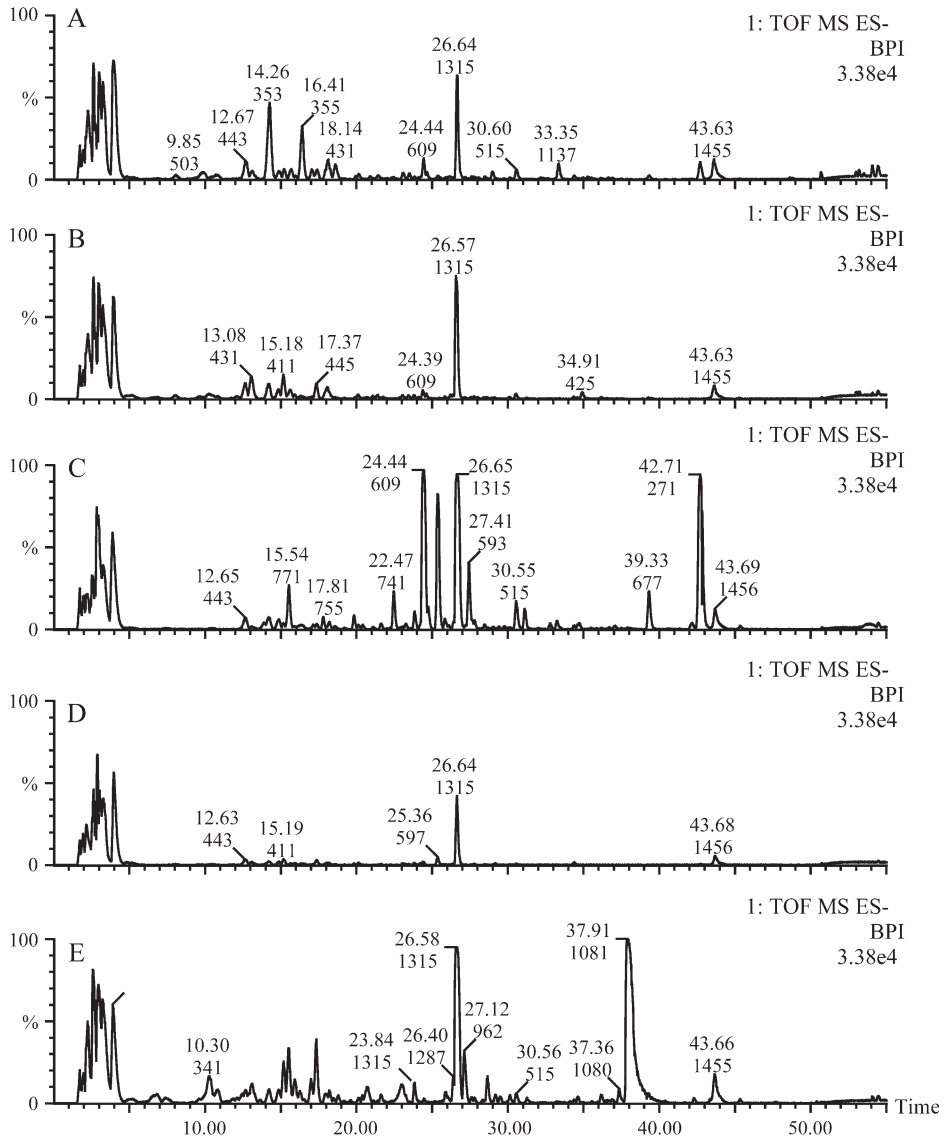

Fig. 3. LC-ESI⁻-QTOF-MS chromatograms of the tissues VAR (A), CP (B), EP (C), PR (D), and JE (E) in red fruits of tomato fruit *Ever* (see Fig. 2 for tissue abbreviations).

Downloaded from https://academic.oup.com/jxb/article/58/15-16/4131/449422 by U.S. Department of Justice user on 17 August 2022

From principal components analyses of these LC-MS profiles (Fig. 4), it appeared that metabolite differences between tissues were more pronounced than differences between ripening stages. The largest metabolite changes were observed between EP and JE, which corresponded to the first principal component in the PCA plot. The second and third components, in contrast, corresponded to fruit development. During ripening, the differences between tissues became more pronounced, suggesting ripening-dependent tissue differentiation related to metabolites.

Quantification of compounds could not be performed in these analyses, as most of the compounds detected are not commercially available as standards. However, compounds identified using LC-PDA-MS/MS in the analysed tissues are listed in Table 2. The performance of the LC-PDA-MS system and the results obtained in this study are in accordance with previous findings (Moco *et al*., 2006), indicating the robustness of the method. Some of the compounds reported in Table 2 have been detected previously in tomato peel and are already present in the MoTo DB. The analysis of different fruit tissues enabled a complementation of the previously putative identifications with additional or improved experimental data, in addition to proposals for newly-found compounds.

Phenolic acids and derivatives thereof

Conjugated forms of caffeic acid, coumaric acid (most likely *p*-coumaric acid), and ferulic acid were detected as relatively high signals in all tissues of tomato fruit. Three isomers of caffeic acid-hexose, eluting at 10.27, 10.88, and 13.19 min, were present in all fruit tissues. These compounds, and in particular the first eluting isomer, were most abundant in the JE and highest at the turning and pink stages of ripening. The second isomer (10.88 min) was almost uniquely present in the VAR. Four isomers of coumaric acid-hexose were found in tomato fruit, eluting at 10.47, 13.90, 14.26, and 15.39 min. The first and fourth isomers were most abundant in the JE, the second in the EP, and the third in the VAR. Three isomers of ferulic acid-hexose, eluting at 12.91, 16.38, and 17.29 min, were also detected and these compounds were highest in the JE (first isomer) or VAR (the second and third isomers).

Three isomers of caffeoylquinic acid were present in all tomato tissues, appearing in the chromatograms at 14.23, 14.86, and 17.18 min. In addition, there were also three isomers of dicaffeoylquinic acids (eluting at 27.82, 28.47, and 30.58 min), as well as three isomers of tricaffeoylquinic acids (appearing at 39.32, 40.63, and 41.35 min) present in all tomato tissues, in particular in the EP, and each of which increased upon fruit ripening.

Flavonoids and derivatives thereof

Flavonoids were typically present in the epidermal tissues. Quercetin, kaempferol, naringenin, and naringenin-chalcone derivatives were found mostly in the EP while some others, such as the aglycones naringenin-chalcone and naringenin and the trisaccharides of kaempferol and quercetin, were mostly present in both EP and VAR. Some flavonoids (e.g. quercetin-dihexose-deoxyhexose, quercetin-hexose-deoxyhexose-pentose-coumaric acid, kaempferol-dihexose-deoxyhexose, naringenin, naringenin chalcone-hexose, and naringenin-dihexose) increased

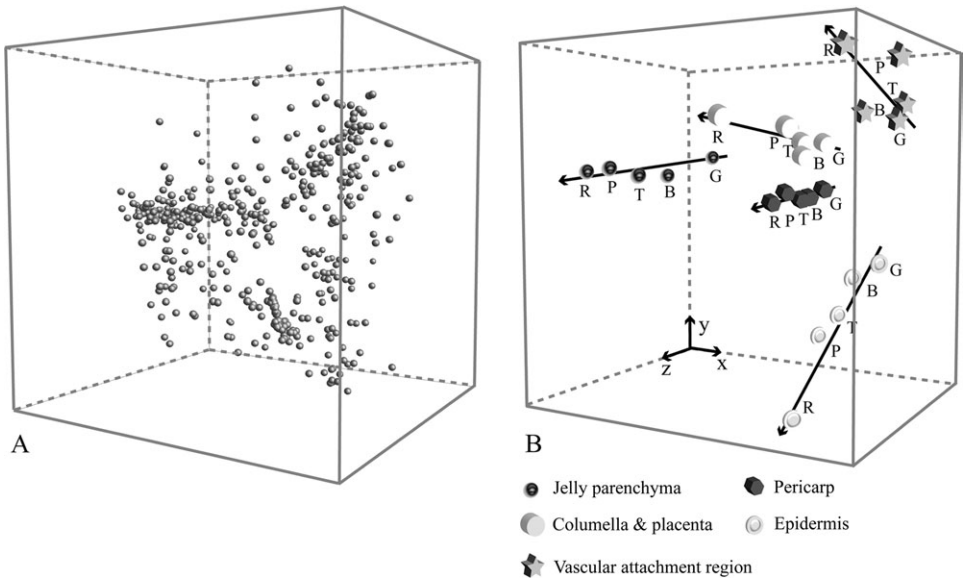

Fig. 4. Principal components analysis (PCA) of LC-ESI$^-$-QTOF-MS data from tomato fruit *Ever* over different ripening stages (G, green; B, breaker; T, turning; P, pink; and R, red) and different tissues within the fruit (VAR, EP, JE, CP, and PR) (see Fig. 2 for tissue abbreviations). PCA plot of the mass signals (A) and of the samples (B) with an explained variance over the *x*-axis (1st principal component, PC1) of 33.6%, *y*-axis (2nd principal component, PC2) of 22.2%, and *z*-axis (3rd principal component, PC3) of 13.2%.

Downloaded from https://academic.oup.com/jxb/article/58/15-16/4131/449422 by U.S. Department of Justice user on 17 August 2022

Table 2. *Metabolites putatively identified by LC-PDA-ESI⁻-QTOF-MS/MS in tissues of tomato fruit*

Ret (min), averaged retention time, in minutes. Mass, averaged accurate mass ([M-H]⁻), in Da, obtained from signals with an intensity ratio 0.25 <analyte/lock mass <2.0. Δmass (ppm), deviation between the averages of observed and calculated accurate masses, in ppm. UV/Vis, absorbance maxima in the UV/Vis range (not detectable absorbance is represented by '–'). MS/MS, fragments obtained through increased collision energy on indicated parent mass. Metabolite name, common name of putatively identified metabolite. Mol form, molecular formula of the metabolite. MM, molecular monoisotopic mass of the metabolite. () FA, formic acid adduct. (T), metabolite previously described in the MoTo DB. I, II, III, IV, different isomers (only one reported in literature).

Ret (min)	Max intensity	Mass	Δmass (ppm)	UV/Vis	MS/MS	Metabolite name	Mol form	MM
4.82	797	164.0725	4.7		146, 103	Phenylalanine	$C_9H_{11}NO_2$	165.0790
7.38	1071	380.1561	−3.8	–	308, 263, 218, 200, 174, 161, 146, 134	Zeatin hexose	$C_{16}H_{23}N_5O_6$	381.1648
10.27	8816	341.0880	0.6			Caffeic acid-hexose I (**T**)	$C_{15}H_{18}O_9$	342.0951
10.47	2864	325.0930	0.3			Coumaric acid-hexose I (**T**)	$C_{15}H_{18}O_8$	326.1002
10.88	913	341.0884	1.6			Caffeic acid-hexose II (**T**)		
12.67	1081	443.1918	−1.0	–	381, 307, 281, 237, 219, 201, 189, 179, 161, 153, 143, 119, 113, 101, 89	Dehydrophaseic acid-hexose	$C_{21}H_{31}O_{10}$	444.1995
12.91	2077	355.1035	0.0			Ferulic acid-hexose I (**T**)	$C_{16}H_{20}O_9$	356.1107
13.19	2340	341.0879	0.3			Caffeic acid-hexose III (**T**)	$C_{15}H_{18}O_9$	342.0951
13.90	1630	325.0929	0.1		163, 119, 93	Coumaric acid-hexose II (**T**)	$C_{15}H_{18}O_8$	326.1002
14.23	14901	353.0873	−1.3		191	3-Caffeoylquinic acid (**T**)	$C_{16}H_{18}O_9$	354.0951
14.26	1510	325.0935	2.0	–		Coumaric acid-hexose III	$C_{15}H_{18}O_8$	326.1002
14.86	2800	353.0878	−0.1			5-Caffeoylquinic acid (**T**)	$C_{16}H_{18}O_9$	354.0951
15.20	7603	411.1872	0.0	–	249, 161, 101	(iso)pentyl dihexose	$C_{17}H_{32}O_{11}$	412.1945
15.39	286	325.0936	2.1	–	265, 235, 205, 163, 145, 117	Coumaric acid-hexose IV	$C_{15}H_{18}O_8$	326.1002
15.55	7842	771.1989	−0.1			Quercetin-dihexose-deoxyhexose (**T**)	$C_{33}H_{40}O_{21}$	772.2062
15.89	631	595.1660	−1.4		549, 475, 433, 415, 385, 355, 313, 271, 263	Naringenin dihexose (**T**)	$C_{27}H_{32}O_{15}$	596.1741
16.38	9995	355.1038	1.0			Ferulic acid-hexose II (**T**)	$C_{16}H_{20}O_9$	356.1107
17.18	2280	353.0876	−0.6			4-Caffeoylquinic acid (**T**)	$C_{16}H_{18}O_9$	354.0951
17.29	1312	355.1031	−0.9	297sh, 329	193, 175, 160, 132	Ferulic acid-hexose III	$C_{16}H_{20}O_9$	356.1107
17.83	2177	755.2036	−0.6	264, 349	593, 447, 285	Kaempferol-dihexose-deoxyhexose	$C_{33}H_{40}O_{20}$	756.2113
20.40	1396	1272.5891	2.0			(Esculeoside B) FA (**T**)	$C_{57}H_{95}NO_{30}$	1273.5939
22.47	16993	741.1946	8.4			Quercetin-hexose-deoxyhexose-pentose (**T**)	$C_{32}H_{38}O_{20}$	742.1956
23.85	3619	1314.5978	0.5			(Lycoperoside F) FA or (Lycoperoside G) FA or (Esculeoside A) FA I (**T**)	$C_{59}H_{97}NO_{31}$	1315.6045
24.14	232	1094.5459	6.4	–	1049, 917, 887, 754, 736, 718, 700, 688, 609, 592, 395, 305, 143, 89	(Lycoperoside H) FA I	$C_{51}H_{85}NO_{24}$	1095.5462
24.44	33024	609.1459	−0.4			Rutin (**T**)	$C_{27}H_{30}O_{16}$	610.1534
24.76	7396	725.1936	0.2	264, 345	593, 575, 285, 255	Kaempferol-hexose-deoxyhexose-pentose	$C_{32}H_{38}O_{19}$	726.2007
25.50	737	1094.5419	2.8	–	1049, 917, 887, 754, 688, 592, 455, 305, 143	(Lycoperoside H) FA II	$C_{51}H_{85}NO_{24}$	1095.5462
25.70	353	425.1821	1.0	–	263, 153	Abscisic acid-hexose	$C_{21}H_{30}O_9$	426.1890
25.83	980	1314.5954	−1.4			(Lycoperoside F) FA or (Lycoperosyde G) FA or (Esculeoside A) FA II (**T**)	$C_{59}H_{97}NO_{31}$	1315.6045
25.87	2053	1312.5817	0.2			(Dehydrolycoperoside F) FA or (Dehydrolycoperoside G) FA or (Dehydroesculeoside A) FA I (**T**)	$C_{59}H_{95}NO_{30}$	1313.5888
26.54	2044	1094.5397	0.7	–	1049, 917, 887, 754, 688, 592, 179, 143, 125	(Lycoperoside H)FA III	$C_{51}H_{85}NO_{24}$	1095.5462
26.62	695	1312.5881	5.0	–	1267, 1137, 1107, 975, 944, 812, 746, 650, 275, 143	(Dehydrolycoperoside F) FA or (Dehydrolycoperoside G) FA or (Dehydroesculeoside A) FA II	$C_{59}H_{95}NO_{30}$	1313.5888
26.62	32144	1314.6003	2.4			(Lycoperoside F) FA or (Lycoperoside G) FA or (Esculeoside A) FA III (**T**)	$C_{59}H_{97}NO_{31}$	1315.6045
27.31	537	1094.5421	3.0			(Lycoperoside H) FA IV (**T**)	$C_{51}H_{85}NO_{24}$	1095.5462
27.45	16802	593.1514	0.3			Kaempferol-3-O-rutinoside (**T**)	$C_{27}H_{30}O_{15}$	594.1585

Downloaded from https://academic.oup.com/jxb/article/58/15-16/4131/449422 by U.S. Department of Justice user on 17 August 2022

Table 2. (*Continued*)

Ret (min)	Max intensity	Mass	Δmass (ppm)	UV/Vis	MS/MS	Metabolite name	Mol form	MM
27.60	1810	1312.5843	2.1	–	1267	(Dehydrolycoperoside F) FA or (Dehydrolycoperoside G) FA or (Dehydroesculeoside A) FA III	$C_{59}H_{95}NO_{30}$	1313.5888
27.62		1314.5920	1.8	–		(Lycoperoside F) FA or (Lycoperosyde G) FA or (Esculeoside A) FA IV	$C_{59}H_{97}NO_{31}$	1315.6045
27.82	1662	515.1199	0.8			Dicaffeoylquinic acid I (**T**)	$C_{25}H_{24}O_{12}$	516.1268
28.47	868	515.1199	0.7			Dicaffeoylquinic acid II (**T**)	$C_{25}H_{24}O_{12}$	516.1268
30.58	4972	515.1193	−0.5			Dicaffeoylquinic acid III (**T**)	$C_{25}H_{24}O_{12}$	516.1268
31.13	3614	887.2255	0.4	258, 321		Quercetin-hexose-deoxyhexose-pentose-*p*-coumaric acid (**T**)	$C_{41}H_{44}O_{22}$	888.2324
32.19	3517	1076.5283	0.0	–	1031, 899, 868, 736, 670, 574, 305, 143, 119, 113	(α-Dehydrotomatin)FA I	$C_{51}H_{83}NO_{23}$	1077.5356
32.75	380	1136.5520	2.2	–		(Lycoperoside A) FA or (Lycoperoside B) FA or (Lycoperoside C) FA I	$C_{53}H_{87}NO_{25}$	1137.5567
32.82	1081	433.1141	0.2			Naringenin chalcone-hexose (**T**)	$C_{21}H_{22}O_{10}$	434.1213
32.84	1960	1078.5451	1.1	–		(α-Tomatin)FA I	$C_{51}H_{85}NO_{23}$	1079.5512
33.31	686	1076.5309	2.4	–		(α-Dehydrotomatin) FA II	$C_{51}H_{83}NO_{23}$	1077.5356
33.33	33734	1078.5438	−0.1		1033, 901, 870, 738, 672, 576, 305, 143, 119, 113	(α-Tomatin) FA II (**T**)	$C_{51}H_{85}NO_{23}$	1079.5512
33.35	23219	1136.5489	−0.4		1092, 959, 929, 796, 731, 634	(Lycoperoside A) FA or (Lycoperoside B) FA or (Lycoperoside C) FA II (**T**)	$C_{53}H_{87}NO_{25}$	1137.5567
33.46	2614	433.1143	0.6			Naringenin chalcone-hexose II (**T**)	$C_{21}H_{22}O_{10}$	434.1213
34.09	918	1136.5505	0.9	–		(Lycoperoside A) FA or (Lycoperoside B) FA or (Lycoperoside C) FA III	$C_{53}H_{87}NO_{25}$	1137.5567
37.94	33859	1081.5448	1.1	–	1037, 919, 903, 757, 740, 595, 161	Tomatoside A	$C_{51}H_{86}O_{24}$	1082.5509
39.32	7103	677.1519	1.0			Tricaffeoylquinic acid I (**T**)	$C_{34}H_{30}O_{15}$	678.1585
40.63	145	677.1533	−3.1			Tricaffeoylquinic acid II (**T**)	$C_{34}H_{30}O_{15}$	678.1585
41.35	112	677.1533	−3.1	–	515, 353	Tricaffeoylquinic acid III	$C_{34}H_{30}O_{15}$	678.1585
42.17	5885	271.0621	3.4			Naringenin (**T**)	$C_{15}H_{12}O_5$	272.0685
42.73	34406	271.0622	3.6			Naringenin chalcone (**T**)	$C_{15}H_{12}O_5$	272.0685

during development, while quercetin-hexose-deoxyhexose-pentose decreased. Rutin and naringenin chalcone were the most abundant flavonoids in the fruit, exhibiting intense mass signals in the EP extracts. It has been reported that these flavonoids increase during fruit development (Bovy *et al*., 2002). However, in the present study an increase of these flavonoids was only observed from the green to the breaker stage, followed by stabilization of their levels up to the red stage. Two glycosylated derivatives of kaempferol, namely kaempferol-rutinoside and kaempferol-hexose-deoxyhexose-pentose, exhibited non-linear patterns during development. The first derivative increased from breaker to red stage, after a decrease from the green to the breaker stage. The second decreased between the green and turning stages, increased again to the pink stage, and returned to lower intensities at the red stage. The ripening and tissue-distribution profiles of the flavonoids rutin, naringenin and naringenin chalcone were confirmed by LC-PDA analyses (data not shown).

Glycoalkaloids

A variety of glycoalkaloids, in ESI^- detected as their formic acid adducts (Moco *et al*., 2006), were present in different tissues and at specific developmental stages. Esculeoside B, eluting at a retention time of 20.40 min, mainly occurred in the JE and its signal intensity slightly decreased during fruit ripening (1.4-fold from green to red stage). Four isomers of lycoperoside H were detected in tomato fruit, at retention times of 24.14, 25.50, 26.54, and 27.31 min. All of these were present essentially in the EP and at highest levels at the early stages of ripening (green and breaker). The alkaloids lycoperoside F and G and esculeoside A have the same molecular mass which appeared four times in the LC-MS chromatogram, suggesting four different isomers (at 23.85, 25.83, 26.62, and 27.62 min). These compounds were present in all tissues and in particular in the EP and JE, but hardly occurred in the green fruit stage. At the red stage, the third isomer was present as one of the highest signals in the mass chromatograms. Three derivatives of lycoperosides

Downloaded from https://academic.oup.com/jxb/article/58/15-16/4131/449422 by U.S. Department of Justice user on 17 August 2022

F and G or esculeoside A, with a mass difference of 2 Da, and therefore recently suggested to be named as dehydrolycoperosides F and G or dehydroesculeoside A (Moco *et al*., 2006), were detected in all tomato fruit tissues. These metabolites had lower signal intensities than the lycoperosides F and G or esculeoside A isomers, but displayed similar tissue distribution and response upon ripening. The last dehydro isomer, eluting at 27.60 min, was only present in the EP and increased more than 1500-fold from the green (below the detection limit) to the red stage. The best known tomato alkaloids, α-tomatin and dehydrotomatin, occurred as two different isomers in all tissues at the green stage, being highest in the EP and JE, and decreasing towards levels below the detection limit at the red stage of development. For both compounds, one isomer was more abundant than the other: the first eluting isomer of dehydrotomatin, retention time 32.19 min (more than 110-fold decrease from green to red) and the second eluting isomer of α-tomatin, retention time 33.33 min (more than 65-fold decrease from green to red). Three isomers of the equal mass metabolites lycoperosides A, B, and C were found in all tissues, with the second isomer (at 33.35 min) being the most abundant. Analogous to α-tomatin, these alkaloids preferably accumulated in the EP and JE, and were highest at the green stage.

Other metabolites

A large number of metabolites present in the extract appeared in the chromatogram before a retention time of 4 min, as a large and mostly asymmetrical single peak. These are (very) polar metabolites that do not interact with the stationary phase. Amino acids, nucleosides, mono-, di-, and tri-phosphate nucleotides, sugars and organic acids are present in this part of the chromatogram. Phenylalanine was the only amino acid actually separated by our instrumental setup (retention time 4.8 min). This amino acid was present in all fruit tissues, was most abundant in the PR and CP, and slightly increased during development (about 2-fold from green to red).

The metabolite assigned as tomatoside A, a saponin, seemed to be specific for the JE extracts, as it displayed extremely high signals at all stages of development of this tissue. From the analysis of the seeds of *Ever* and *Moneymaker* and their comparison with the gelatinous part of the JE tissue, it appeared that this saponin was highly abundant in the seeds (Fig. 5). These results suggest that this compound may be uniquely present in the seeds. Likewise, a compound with *m/z* 962.5, at 26.2 min, is also present in the seeds and not in the gelatinous part of the JE tissue (Fig. 5), and appears to be a formic acid adduct of an alkaloid-dihexoside. On the other hand, *m/z* 1314.595 at retention time 25.8, annotated as lycoperoside F or G or esculeoside A (Table 2), was not detec table in the isolated seeds.

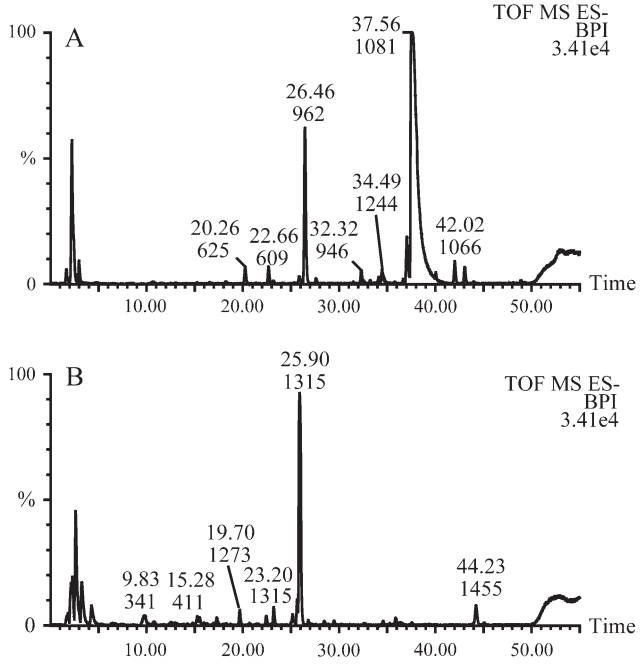

Fig. 5. LC-ESI⁻-QTOF-MS chromatograms of seeds (A) and gelatinous part (B) of the jelly parenchyma (JE) of tomato fruit samples of *Ever* (both 1:10 (v/v) diluted).

Glycosylated hormonal metabolites, zeatin hexose and abscisic acid hexose, were also found in the fruit tissues of cultivar *Ever*, in particular in the JE extracts (excluding seeds). Both metabolites increased during development (up to 8-fold). The metabolite dehydrophaseic acid-hexose, belonging to the abscisic acid pathway, was found in all tissues, including in the seeds, and at all ripening stages, being highest in the red VAR.

Metabolite pattern classification according to tissue and development

To enable grouping of metabolites according to their relative distribution over the samples, the LC-PDA-FI and LC-MS datasets from the analyses of tissues and ripening stages of the tomato variety *Ever* were concatenated. The combined dataset was processed using the Multivariate Mass Spectra Reconstruction method, previously described for gas chromatography-MS data (Tikunov *et al*., 2005). This processing approach grouped the dataset into 14 different pattern clusters. Metabolites which have been previously identified (Tables 1, 2; Moco *et al*., 2006) fitted into nine of these 14 clusters (Fig. 6).

In each cluster, chemically diverse metabolites were grouped, indicating that the clustering was independent of the chemical class of metabolites. By contrast, this pattern analysis led to a biological classification according to tissue and ripening stage. The clusters A, B, and C included metabolites that were relatively high in the EP, present at constant levels (A), increasing (C) or decreasing

Downloaded from https://academic.oup.com/jxb/article/58/15-16/4131/449422 by U.S. Department of Justice user on 17 August 2022

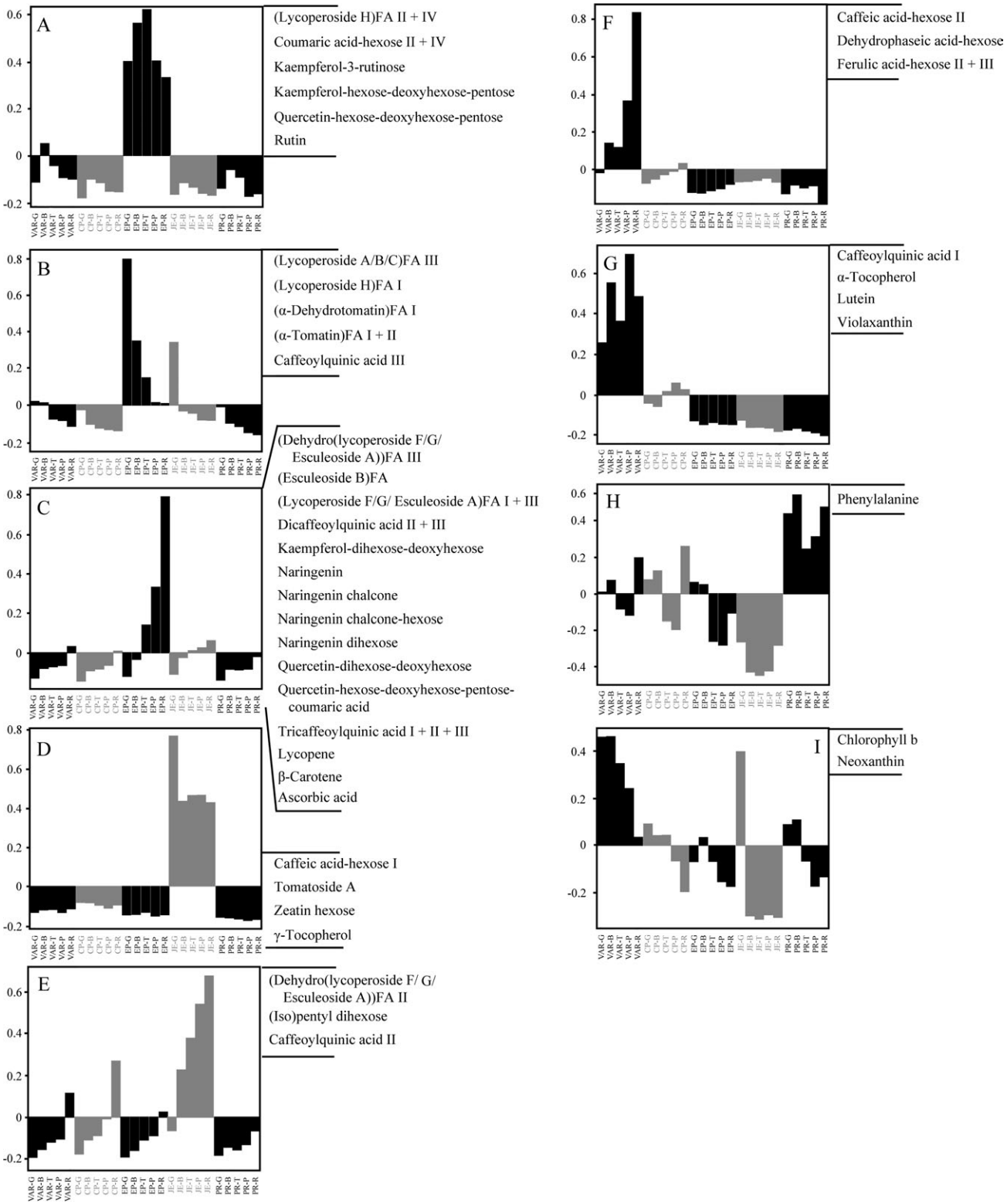

Fig. 6. Classification of metabolite data, according to their relative abundance in tomato fruit tissues of the cultivar *Ever*, along ripening. After range scaling normalization over the intensities of the metabolite signals (intensities in μg g^{-1} dry weight were used for metabolites quantified by LC-PDA-FD and averaged mass signal intensities for metabolites detected by LC-PDA-ESI^--QTOF-MS), the combined dataset was clustered using the Self Organizing Tree Algorithm (SOTA). Plots A, B, C, D, E, F, G, H, and I represent nine clusters, out of a total of 14 recognized clusters obtained by this analysis, containing the (putatively) assigned metabolites (see Tables 1 and 2). The patterns display, from left to right, the different fruit tissues (see Fig. 2 for tissue abbreviations), VAR (VAR, in black), CP (CP, in grey), EP (EP, in black), JE (JE, in grey), and PR (PR, in black); within each tissue, the ripening stages are displayed: green (G), breaker (B), turning (T), pink (P), and red (R).

Downloaded from https://academic.oup.com/jxb/article/58/15-16/4131/449422 by U.S. Department of Justice user on 17 August 2022

(B) upon fruit ripening. In these clusters, flavonoids, phenolic acids and alkaloids were present. The clusters D and E comprise metabolites that are abundant in the JE. Metabolites relatively high in the VAR are grouped in the clusters F, G, and I, while metabolites most abundant in the PR were grouped in cluster H. The mass intensity signals (taken from the LC-MS data) or the quantitative values (μg mg^{-1} dry weight) of each classified metabolite fitted the proposed cluster patterns (see Supplementary Figs S1–S4 at *JXB* online).

Discussion

Tissue specialization during fruit development is an intricate biological process where differentiation at the physical, chemical, and biological levels, take place simultaneously. These changes result in a series of dynamic modifications to the whole metabolic pathway network leading to cell division, cell expansion, biosynthetic specialization, etc, ultimately leading to fruit ripening and, eventually, senescence. The transformation of an ovary into a mature fruit has been the target of intensive studies, regarding practically all aspects of fruit development. In particular, at the early stage of fruit set, the hormonal regulation and the interaction of different hormones have been studied extensively (Gillaspy *et al*., 1993; Giovannoni, 2001). The assignment of genes involved in fruit formation and ripening processes, the analysis of transcripts and proteins, as well as registering alterations to a limited set of known metabolites during development have been previously well documented (Gillaspy *et al*., 1993; Buta and Spaulding, 1997; Srivastava and Handa, 2005). Recently, a comprehensive study on the primary metabolism in developing tomato fruit, using a GC-TOF MS based metabolomics approach, has been performed at both metabolite and transcript levels (Carrari *et al*., 2006). However, so far, tissue differentiation during fruit formation and maturation has been monitored mostly at the morphological level and much less at the biochemical level. In the present study, the (relative) abundance of a large number of metabolites present in specific fruit tissues was followed during ripening using LC-PDA-FD- and LC-PDA-QTOF-MS-based metabolomics approaches. Most of the metabolites detected by these approaches form part of the plant's secondary metabolism and therefore, are generally believed not to be involved in vital plant processes but rather, confer biotic or abiotic stress resistance, taste, fragrance, etc.

The LC-MS analyses of the peel and flesh tissues from several different commercial tomato cultivars and the subsequent principal components analysis indicated that tissue specificity was the major factor determining the differences in metabolic profiles between samples (Fig. 1). These findings suggest the presence of common metabolites localized in the same tissue among all cultivars, irrespective of the different genetic backgrounds of the fruits. Furthermore, the presence of certain metabolites specifically accumulating in particular tissues provides information about metabolite localization and tissue specificity within the tomato fruit.

The observed loss of rigidity during ripening has been well documented. This softening involves physicochemical changes occurring in the fruit cell walls, involving modifications in cell wall polymers, mainly due to enzymatic hydrolysis of pectin (Carrari *et al*., 2006; Tomassen *et al*., 2007). The alteration of fruit size during development is minor and almost irrelevant after the green stage, as the fruit size appears stable (Giovannoni, 2001). Therefore, all changes reported here are related specifically to the post-expansion phase of fruit development.

The pigmentation of the tomato fruit is due to the presence of light-absorbing metabolites such as chlorophylls, carotenoids, and certain flavonoids. The green colour of the tissues in the early stages of development is caused by the presence of chlorophylls. In tomato, both chlorophyll *a* and *b*, differing in an aldehyde group (in chlorophyll *b*) instead of a methyl group (in chlorophyll *a*) are detected. These two related metabolites complement each other in their photoreception capabilities, enlarging the light-absorbing spectrum. At each ripening stage the level of total chlorophylls was the highest in the VAR and the lowest in the EP. There is evidence (Smillie *et al*., 1999) indicating that the chlorophylls present are photosynthetically active in all tissues of the fruit including the VAR and even inner tissues such as the JE. The same authors suggested that the photosynthetic capacity of the JE might be of importance in the development and maturation of the seeds. The presence of chlorophylls in the inner fruit layers of the tomato fruit is in accordance with the transcriptional patterns of chlorophyll *a/b* related proteins, which were found to be preferentially expressed in the locular fruit tissue (Lemaire-Chamley *et al*., 2005).

The transformation of chloroplasts into chromoplasts during fruit ripening is paired with the degradation of chlorophylls and the synthesis of carotenoids, in particular all-*trans* lycopene. Lycopene is the pigment typically conferring the red colour of ripe tomato fruits and which accumulates in fruit cell-localized phytochromes. These organelles determine the colour development in tomato by controlling the amount of accumulated lycopene (Alba *et al*., 2000). Lycopene is present in all fruit tissues, although highest levels were detected in the EP. Carotenoids in general, play an attractant role for seed dispersal and therefore can influence the further propagation of the species. The observed profiles of carotenoids in tomato fruit during ripening are comparable to other studies (Fraser *et al*., 1994), where a different cultivar was used. The main carotenoids detected (neoxanthin, violaxanthin,

Downloaded from https://academic.oup.com/jxb/article/58/15-16/4131/449422 by U.S. Department of Justice user on 17 August 2022

β-carotene, lycopene, and lutein) are present in all tissues of the fruit, including the inner parts of the fruit such as the JE.

LC-MS analysis of tomato fruit tissues can provide important information about the tissue distribution of semi-polar metabolites and their fate upon ripening. From these analyses, it became clear that most metabolites are not equally distributed across the fruit, but rather, show preferential accumulation in one or more specific tissues. Moreover, variation in metabolites between tissues was more pronounced than the variation induced by ripening, which was the second cause of profile segregation.

At all ripening stages, the most extreme differences with regard to metabolite composition were observed between the EP and JE. Glycosylated flavonoids, including rutin, kaempferol rutinoside, and a quercetin trisaccharide (i.e. quercetin-hexose-deoxyhexose-pentose), were found to be specifically abundant in the EP and were present either at similar levels at all developmental stages or accumulated upon ripening. Deglycosylated flavonoids are especially known for their capacity for electron transfer, as anti-oxidants and also as pro-oxidants (Awad *et al*., 2001; Lemanska *et al*., 2001). As such, flavonoids can participate as plant protective elements in both biotic and abiotic phenomena such as defence against pathogens and environmental stress involving, for example, drought, UV radiation, and wounding (Pourcel *et al*., 2007). In addition, flavonoids have been associated with auxin transport in the plant, acting as endogenous mediators of auxin flow (Besseau *et al*., 2007). During fruit development, high levels of naringenin chalcone accumulate in the EP. Also, multiple glycosylated forms of flavonoids (dihexose-deoxyhexoses of kaempferol and quercetin) increase in concentration during development, possibly due to the increase in the production of sugars and therefore, in higher conjugation possibilities. The presence of flavonoid derivatives in the outer fruit layers of tomato is in accordance with the fact that the transcription of genes involved in flavonoid biosynthesis, including phenylalanine ammonia-lyase, flavanone 3-hydroxylase, flavonol synthase, and sugar transporters, is higher in the exocarp tissues than in the inner locular tissue (Lemaire-Chamley *et al*., 2005). Likewise, the antioxidant ascorbic acid increases in the fruit upon ripening and is particularly high in the EP. By acting as a major electron transfer component in numerous reactions, ascorbic acid is likely to be involved in vital plant processes such as hormone biosynthesis (e.g. abscisic acid), detoxification of reactive oxygen species, regeneration of isoprenoid derivatives (e.g. α-tocopherol, zeaxanthin) and consequently, photosynthetic activity and plant growth (Chen and Gallie, 2006). In agreement with the authors' findings that ascorbic acid levels are relatively high in the EP, the transcript level of guanidine diphosphate-mannose pyrophosphorylase, an enzyme involved in ascorbic acid biosynthesis, was also found to be higher in the exocarp than in the locular tissue (Lemaire-Chamley *et al*., 2005).

The JE material (including the seeds) is relatively rich in specific semi-polar metabolites. The locular tissue surrounding the seeds is of importance to the maturation of seeds during fruit development, and the presence of hormonal compounds in this tissue suggests that the cellular environment surrounding the seeds is subjected to hormonal regulation processes (Gillaspy *et al*., 1993). In fact, abscisic acid is involved in seed dormancy phenomena, which may explain the presence of abscisic acid pathway-related metabolites such as dehydrophaseic acid-hexose and absisic acid-hexose in the JE extracts. Relative high levels of abscisic acid-hexose were detected in the gelatinous part (without seeds) of the JE, as well as of the glycosylated cytokinin, zeatin-hexose, that increased in concentration during fruit ripening. The latter finding is in agreement with the preferential expression of the zeatin-*O*-glucosyltransferase gene in the locular tissue (Lemaire-Chamley *et al*., 2005). The increase of glycosylated hormonal metabolites during fruit development is in accordance with the discontinued need of hormonal (non-glycosylated) triggering molecules, such as abscisic acid and zeatin, after the cell expansion of the fruit (prior to the mature green stage) (Gillaspy *et al*., 1993). In addition to these plant hormones, the saponin tomatoside A was specifically present in the seeds of tomato. However, no biological function has yet been assigned to this compound.

A class of compounds that exhibited marked developmental features are the glycoalkaloids. Glycoalkaloids such as tomatine are proposed to be formed through the cholesterol pathway, in which a series of modifications takes place to the steroid moiety. During the last biosynthesis step, the steroid tomatidine is glycosylated into α-tomatine (Friedman, 2002). The green fruit-specific metabolites α-tomatine and dehydrotomatine could be detected in all fruit tissues, but were specifically abundant in the EP. Both alkaloids strongly decreased at the first signs of fruit ripening. By contrast, several other alkaloids, also preferentially accumulating in the EP, markedly increased upon ripening: lycoperosides F and G and esculeoside A and their dehydro forms dehydrolycoperosides F, G, and dehydroesculeoside A. Esculeoside A has been postulated to be formed from α-tomatine, through a ring rearrangement in the steroid moiety (Fujiwara *et al*., 2004). The functions of all these alkaloids in plants are, however, still not fully understood. Some glycoalkaloids are known to have antimicrobial and insecticidal properties, allelopathic activity, and they participate in plant defence mechanisms (Friedman, 2002). The antifungal activity of both α-tomatine and its aglycon tomatidine has been recently studied (Simons *et al*., 2006). α-Tomatine can easily pass through the fungal cell membrane, however, it has lower antifungal activity compared with

Downloaded from https://academic.oup.com/jxb/article/58/15-16/4131/449422 by U.S. Department of Justice user on 17 August 2022

tomatidine, suggesting that the sugar moiety is important for cell penetration while the steroid moiety confers toxicity to the fungus. Upon internalization, α-tomatine is recognized by enzymes produced by fungal pathogens which can hydrolyse one sugar unit or even the complete sugar moiety to yield tomatidine. Based on fungal gene expression data, tomatidine (but not α-tomatine) inhibits ergosterol biosynthesis, which is also a key target for chemical control of fungal pathogens of plants and animals (Simons *et al*., 2006).

Conclusion

Tomato fruit ripening involves a complex set of unique biological processes with the regulation of metabolic pathways taking place within specific tissues of the fruit. In the present study, an extensive biochemical characterization of different fruit tissues, at different ripening stages, was performed through LC-based metabolomics approaches biased towards secondary metabolites. Many of the metabolites detected were not uniformly distributed over the tomato fruit upon ripening, but rather, preferentially accumulated in specific fruit tissue(s) as well as at specific ripening stage(s). This information adds to our understanding of tempo-spatial differentiation of metabolic pathways during fruit development. Future studies, for example, by using fruits from other genotypes and natural or induced mutants, might also be performed to confirm the observed tissue-preference of metabolites and to give more insight into the tissue-specific regulation of metabolic pathways and the biological function of (secondary) metabolites.

Acknowledgements

This study was financed by the research programme of the Centre of BioSystems Genomics (CBSG) which is a part of The Netherlands Genomics Initiative/Netherlands Organization for Scientific Research, the EU project 'META-PHOR', contract number FOOD-CT-2006-036220 and the EU project 'FLORA', contract number FOOD-CT-2005-007130.

The authors would like to thank several colleagues at Plant Research International, Wageningen, for their important contribution to this work: Harry Jonker and Bert Schipper for taking care that the instruments were up and running and for their help in sample extraction and analyses, Dr Tom Dueck for kindly providing the fruits from the cultivar *Ever*, Dr Arnaud Bovy for his significant input in the fruitful discussions on the results, and Dr Jules Beekwilder.

Supplementary data

Mass signal intensities of (putatively) assigned metabolites (see Tables I and II) from the LC-PDA-FD and LC-MS analyses of the fruit tissues of tomato cultivar *Ever* are presented in the Supplementary Figs S1–S4.

References

Alba R, Cordonnier-Pratt MM, Pratt LH. 2000. Fruit-localized phytochromes regulate lycopene accumulation independently of ethylene production in tomato. *Plant Physiology* **123,** 363–370.

Awad HM, Boersma MG, Boeren S, van Bladeren PJ, Vervoort J, Rietjens I. 2001. Structure–activity study on the quinone/quinone methide chemistry of flavonoids. *Chemical Research in Toxicology* **14,** 398–408.

Basu A, Imrhan V. 2007. Tomatoes versus lycopene in oxidative stress and carcinogenesis: conclusions from clinical trials. *European Journal of Clinical Nutrition* **61,** 295–303.

Besseau S, Hoffmann L, Geoffroy P, Lapierre C, Pollet B, Legrand M. 2007. Flavonoid accumulation in Arabidopsis repressed in lignin synthesis affects auxin transport and plant growth. *The Plant Cell* **19,** 148–162.

Bino RJ, De Vos RCH, Lieberman M, Hall RD, Bovy A, Jonker HH, Tikunov Y, Lommen A, Moco S, Levin I. 2005. The light-hyperresponsive *high pigment-2^{dg}* mutation of tomato: alterations in the fruit metabolome. *New Phytologist* **166,** 427–438.

Bovy A, De Vos RCH, Kemper M, *et al*. 2002. High-flavonol tomatoes resulting from the heterologous expression of the maize transcription factor genes LC and C1. *The Plant Cell* **14,** 2509–2526.

Buta JG, Spaulding DW. 1997. Endogenous levels of phenolics in tomato fruit during growth and maturation. *Journal of Plant Growth Regulation* **16,** 43–46.

Carrari F, Baxter C, Usadel B, *et al*. 2006. Integrated analysis of metabolite and transcript levels reveals the metabolic shifts that underlie tomato fruit development and highlight regulatory aspects of metabolic network behavior. *Plant Physiologyt* **142,** 1380–1396.

Chen Z, Gallie DR. 2006. Dehydroascorbate reductase affects leaf growth, development, and function. *Plant Physiology* **142,** 775–787.

Choi C, Munch R, Leupold S, *et al*. 2007. SYSTOMONAS: an integrated database for systems biology analysis of *Pseudomonas*. *Nucleic Acids Research* **35,** D533–D537.

De Vos RCH, Moco S, Lommen A, Keurentjes JJB, Bino RJ, Hall RD. 2007. Untargeted large-scale plant metabolomics using liquid chromatography coupled to mass spectrometry. *Nature Protocols* **2,** 778–791.

Ellis DI, Goodacre R. 2006. Metabolic fingerprinting in disease diagnosis: biomedical applications of infrared and Raman spectroscopy. *Analyst* **131,** 875–885.

FAOSTAT. 2005. *FAOSTAT statistics division*. FAOSTAT/Food and Agriculture Organization of the United Nations. Vol. 2007 .

Fraser PD, Enfissi EMA, Goodfellow M, Eguchi T, Bramley PM. 2007. Metabolite profiling of plant carotenoids using the matrix-assisted laser desorption ionization time-of-flight mass spectrometry. *The Plant Journal* **49,** 552–564.

Fraser PD, Truesdale MR, Bird CR, Schuch W, Bramley PM. 1994. Carotenoid biosynthesis during tomato fruit development (evidence for tissue-specific gene expression). *Plant Physiology* **105,** 405–413.

Friedman M. 2002. Tomato glycoalkaloids: role in the plant and in the diet. *Journal of Agricultural and Food Chemistry* **50,** 5751–5780.

Fujiwara Y, Takaki A, Uehara Y, Ikeda T, Okawa M, Yamauchi K, Ono M, Yoshimitsu H, Nohara T. 2004. Tomato steroidal alkaloid glycosides, esculeosides A and B, from ripe fruits. *Tetrahedron* **60,** 4915–4920.

Gillaspy G, Bendavid H, Gruissem W. 1993. Fruits: a developmental perspective. *The Plant Cell* **5,** 1439–1451.

Downloaded from https://academic.oup.com/jxb/article/58/15-16/4131/449422 by U.S. Department of Justice user on 17 August 2022

Giovannoni J. 2001. Molecular biology of fruit maturation and ripening. *Annual Review of Plant Physiology and Plant Molecular Biology* **52,** 725–749.

Griffin JL, Kauppinen RA. 2007. A metabolomics perspective of human brain tumours. *FEBS Journal* **274,** 1132–1139.

Hall RD. 2006. Plant metabolomics: from holistic hope, to hype, to hot topic. *New Phytologist* **169,** 453–468.

Herrero J, Valencia A, Dopazo J. 2001. A hierarchical unsupervised growing neural network for clustering gene expression patterns. *Bioinformatics* **17,** 126–136.

Horwitz W. 2000. *Official methods of analysis of AOAC International*. Maryland: AOAC International.

Jatoi A, Burch P, Hillman D, *et al*. 2007. A tomato-based, lycopene-containing intervention for androgen-independent prostate cancer: results of a Phase II study from the North Central Cancer Treatment Group. *Urology* **69,** 289–294.

Keun HC, Ebbels TMD, Antti H, *et al*. 2002. Analytical reproducibility in H-1 NMR-based metabonomic urinalysis. *Chemical Research in Toxicology* **15,** 1380–1386.

Kochhar S, Jacobs DM, Ramadan Z, Berruex F, Fuerhoz A, Fay LB. 2006. Probing gender-specific metabolism differences in humans by nuclear magnetic resonance-based metabonomics. *Analytical Biochemistry* **352,** 274–281.

Kopka J, Schauer N, Krueger S, *et al*. 2005. GMD@CSB.DB: the Golm Metabolome Database. *Bioinformatics* **21,** 1635–1638.

Kunz BA, Cahill DM, Mohr PG, Osmond MJ, Vonarx EJ. 2006. Plant responses to UV radiation and links to pathogen resistance. In: Jeon KW, ed. *A survey of cell biology, International Review of Cytology*, Vol. 255. Academic Press, 1–40.

Le Gall G, Colquhoun IJ, Davis AL, Collins GJ, Verhoeyen ME. 2003. Metabolite profiling of tomato (*Lycopersicon esculentum*) using ^{1}H NMR spectroscopy as a tool to detect potential unintended effects following a genetic modification. *Journal of Agricultural and Food Chemistry* **51,** 2447–2456.

Lemaire-Chamley M, Petit J, Garcia V, Just D, Baldet P, Germain V, Fagard M, Mouassite M, Cheniclet C, Rothan C. 2005. Changes in transcriptional profiles are associated with early fruit tissue specialization in tomato. *Plant Physiology* **139,** 750–769.

Lemanska K, Szymusiak H, Tyrakowska B, Zielinski R, Soffers AEMF, Rietjens IMCM. 2001. The influence of pH on antioxidant properties and the mechanism of antioxidant action of hydroxyflavones. *Free Radical Biology and Medicine* **31,** 869–881.

Moco S, Bino RJ, Vorst O, Verhoeven HA, de Groot J, van Beek TA, Vervoort J, De Vos RCH. 2006. A liquid chromatography–mass spectrometry-based metabolome database for tomato. *Plant Physiology* **141,** 1205–1218.

Ogata H, Goto S, Sato K, Fujibuchi W, Bono H, Kanehisa M. 1999. KEGG: Kyoto encyclopedia of genes and genomes. *Nucleic Acids Research* **27,** 29–34.

Oikawa A, Nakamura Y, Ogura T, Kimura A, Suzuki H, Sakurai N, Shinbo Y, Shibata D, Kanaya S, Ohta D. 2006. Clarification of pathway-specific inhibition by Fourier transform ion cyclotron resonance/mass spectrometry-based metabolic phenotyping studies. *Plant Physiology* **142,** 398–413.

Porter SEG, Stoll DR, Rutan SC, Carr PW, Cohen JD. 2006. Analysis of four-way two-dimensional liquid chromatography-diode array data: application to metabolomics. *Analytical Chemistry* **78,** 5559–5569.

Pourcel L, Routaboul JM, Cheynier V, Lepiniec L, Debeaujon I. 2007. Flavonoid oxidation in plants: from biochemical properties to physiological functions. *Trends in Plant Science* **12,** 29–36.

Schauer N, Fernie AR. 2006. Plant metabolomics: towards biological function and mechanism. *Trends in Plant Science* **11,** 508–516.

Schauer N, Steinhauser D, Strelkov S, *et al*. 2005. GC-MS libraries for the rapid identification of metabolites in complex biological samples. *FEBS Letters* **579,** 1332–1337.

Simons V, Morrissey JP, Latijnhouwers M, Csukai M, Cleaver A, Yarrow C, Osbourn A. 2006. Dual effects of plant steroidal alkaloids on *Saccharomyces cerevisiae*. *Antimicrobial Agents and Chemotherapy* **50,** 2732–2740.

Smilde AK, van der Werf MJ, Bijlsma S, van der Werff-van-der Vat BJC, Jellema RH. 2005. Fusion of mass spectrometry-based metabolomics data. *Analytical Chemistry* **77,** 6729–6736.

Smillie RM, Hetherington SE, Davies WJ. 1999. Photosynthetic activity of the calyx, green shoulder, pericarp, and locular parenchyma of tomato fruit. *Journal of Experimental Botany* **50,** 707–718.

Srivastava A, Handa AK. 2005. Hormonal regulation of tomato fruit development: a molecular perspective. *Journal of Plant Growth Regulation* **24,** 67–82.

Taylor LP, Grotewold E. 2005. Flavonoids as developmental regulators. *Current Opinion in Plant Biology* **8,** 317–323.

Tikunov Y, Lommen A, De Vos RCH, Verhoeven HA, Bino RJ, Hall RD, Bovy AG. 2005. A novel approach for nontargeted data analysis for metabolomics. Large-scale profiling of tomato fruit volatiles. *Plant Physiology* **139,** 1125–1137.

Tomassen MMM, Barrett DM, van der Valk HCPM, Woltering EJ. 2007. Isolation and characterization of a tomato non-specific lipid transfer protein involved in polygalacturonase-mediated pectin degradation. *Journal of Experimental Botany* **58,** 1151–1160.

Tracewell CA, Vrettos JS, Bautista JA, Frank HA, Brudvig GW. 2001. Carotenoid photooxidation in photosystem II. *Archives of Biochemistry and Biophysics* **385,** 61–69.

van der Werf MJ, Jellema RH, Hankemeier T. 2005. Microbial metabolomics: replacing trial-and-error by the unbiased selection and ranking of targets. *Journal of Industrial Microbiology and Biotechnology* **32,** 234–252.

Ward JL, Harris C, Lewis J, Beale MH. 2003. Assessment of H-1 NMR spectroscopy and multivariate analysis as a technique for metabolite fingerprinting of *Arabidopsis thaliana*. *Phytochemistry* **62,** 949–957.

Wishart DS, Tzur D, Knox C, *et al*. 2007. HMDB: the human metabolome database. *Nucleic Acids Research* **35,** D521–526.

Downloaded from https://academic.oup.com/jxb/article/58/15-16/4131/449422 by U.S. Department of Justice user on 17 August 2022